Phase Diagrams and Interface in Inflating Balloon

Fanlong Meng
State Key Laboratory of Theoretical Physics, Institute of Theoretical Physics, Chinese Academy of Sciences, Beijing 100190, China

Kavli Institute for Theoretical Physics China, Beijing 100190, China

Center of Soft Matter Physics and its Applications, Beihang University, Beijing, China

Jeff Z. Y. Chen
Dept. of Physics and Astronomy, University of Waterloo, Waterloo, ON, Canada N2L3G1

Masao Doi
Center of Soft Matter Physics and its Applications, Beihang University, Beijing, China

Zhongcan Ouyang
State Key Laboratory of Theoretical Physics, Institute of Theoretical Physics, Chinese Academy of Sciences, Beijing 100190, China

Kavli Institute for Theoretical Physics China, Beijing 100190, China

Center for Advanced Study, Tsinghua University, Beijing 100084, China

DOI 10.1002/aic.14410
Published online February 25, 2014 in Wiley Online Library (wileyonlinelibrary.com)

When a cylindrical balloon is inflated, inflation often takes place nonuniformly, inflated near one end first and followed by the growth of this part along the entire cylinder. This phenomenon is discussed from the phase-transition perspective in terms of the Gent model, a free-energy model that has the same structure as that of the gas–liquid transition in normal fluids. A phase diagram which describes the inflation behavior is constructed, showing the binodal and spinodal curves terminated at a critical point. The hysteresis effects are discussed based on the phase diagram. The interface between the coexisting inflated and weakly inflated regions along the cylindrical balloon is also examined, and the interfacial thickness and the interfacial energy are numerically calculated. © 2014 American Institute of Chemical Engineers *AIChE J*, 60: 1393–1399, 2014
Keywords: rheology, phase equilibrium, phase transition, balloon inflation, interface

Introduction

We have known for a long time that a rubber balloon is inflated nonuniformly when air pressure is applied to the opening end. For example, when a cylindrical balloon is inflated, an inflated part appears near one end first with the rest part only weakly inflated; further inflation grows from the already inflated part along the cylinder axis (see Figure 1). This phenomenon, commonly known to all children, has attracted attention of many researchers since the early work of Mallock.[1] The subject matter has been discussed in many fields: physics, mathematics, mechanical engineering, chemical engineering, and so forth.[2–4] A review can be found in Refs. 5,6

It is now known that the nonuniform inflation of balloon is caused by the nonlinear elasticity of the rubber material itself. Using a nonlinear elastic model of rubber, one can show that the pressure in a spherical or a cylindrical balloon becomes a nonmonotonous function of volume. Such a pressure–volume curve suggests a similarity between the current problem and the gas–liquid transition in a fluid.

In this article, we discuss the balloon-inflation problem from the viewpoint of the phase transition theory, particularly using the analogy to the gas–liquid phase transition. The inflated and weakly inflated parts of a cylindrical balloon are identified as two states of a first-order transition. We produce phase diagrams for the inflation behavior based on the Gent energy model, which also allows us to discuss the hysteresis effects in balloon inflation. The interface between the coexisting inflated and weakly inflated regions is analogous to the coexistent gas and liquid states, which is analyzed in detail in this article. Although the balloon inflation problem has been considered previously, the phase diagram in the entire parameter space and the related interfacial properties are addressed for the first time in this article.

Inflation of a Cylindrical Balloon

Pressure vs. volume curve

To discuss the phase properties, here we assume that the cylindrical balloon can be modeled by a long cylinder, which

Correspondence concerning this article should be addressed to M. Doi at masao.doi.octa.pc@gmail.com.

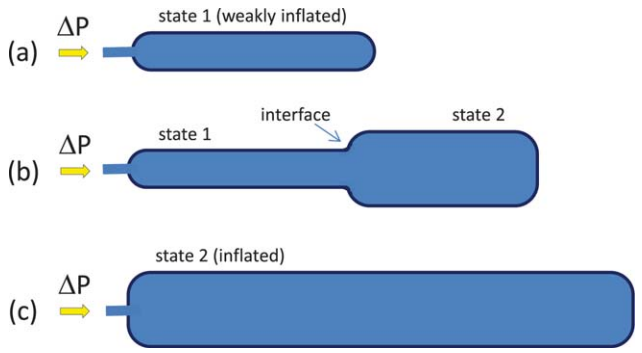

Figure 1. Shape of an inflated cylinder balloon.

Plot (a) shows a weakly inflated balloon at low pressure; plot (b) shows an intermediate stage where two states coexist with an interface; plot (c) shows the final stage in the inflated state. The transition between state 1 and state 2 is identified here as a first-order phase transition. [Color figure can be viewed in the online issue, which is available at wileyonlinelibrary.com.]

has radius R_0 and length L_0 in the force-free state. For simplicity, we ignore the cylinder's end effects, although the current model can be used to include the end effects. The material of the cylinder surface is made of a thin, uniform rubber membrane which has thickness H_0. As a pressure is exerted inside the cylinder, the balloon inflates and the cylinder shape is now described by a uniform radius R, length L, and membrane thickness H. Because the rubber membrane is thin, the bending energy of the membrane is negligible. The entire theory is built on the assumption $H \ll R \ll L$. The case of nonuniform R is considered in interface section.

To discuss the equilibrium shape of the balloon, we consider the free energy of the system. In the present case, this is given by the rubber deformation energy of the balloon. Geometrically, each volume element of the membrane can be stretched along three orthogonal directions, by a factor $\lambda_L \equiv L/L_0$ along the axial direction of the cylinder, by a factor $\lambda_R \equiv R/R_0$ along the circumferential direction, and by a factor $\lambda_H \equiv H/H_0$ along the direction normal to the membrane surface. The incompressibility condition of a polymeric system requires

$$\lambda_L \lambda_R \lambda_H = 1 \tag{1}$$

which is a constraint on the three variables.

The models for the elastic energy per unit volume of rubber, $f(\lambda_R, \lambda_L, \lambda_H)$, have been proposed previously.[7] The most well-known form of $f(\lambda_R, \lambda_L, \lambda_H)$ is the Neo-Hookean model

$$f_{\mathrm{NH}}(\lambda_R, \lambda_L, \lambda_H) = (\mu/2) J_1 \tag{2}$$

where μ is the shear modulus and J_1 is the stretching parameter defined by

$$J_1 = \lambda_R^2 + \lambda_L^2 + \lambda_H^2 - 3 \tag{3}$$

Basically, quadratic energy penalties are proposed along the three deformation directions. Hence, the model is suitable for weak perturbation of the rubber shape against the equilibrium state represented by $\lambda_L = \lambda_R = \lambda_H = 1$

However, the Neo-Hookean model fails to capture the nonlinear nature of the distortion force in large deformation of rubber, in particular the fundamental property that rubber cannot be stretched beyond a given limit. Gent proposed a model that can be used to describe this limiting behavior[8]

$$f_{\mathrm{Gent}} = (\mu/2) f(\lambda_R, \lambda_L) \tag{4}$$

where the dimensionless factor

$$f(\lambda_R, \lambda_L) = -J_{\mathrm{m}} \ln\left(1 - \frac{J_1}{J_{\mathrm{m}}}\right) \tag{5}$$

where J_{m} is a material-dependent parameter representing the limiting value of J_1. The Gent model reduces to the Neo-Hookean model in weak stretching when J_1 is small. As described below, to describe the coexistence between the inflated and weakly inflated phases, it is necessary to use the Gent model to account for large shape distortion.

Following the Gent model, we can then write the total free energy of the system

$$F(\lambda_R, \lambda_L) = \pi R_0 H_0 L_0 \mu f(\lambda_R, \lambda_L) \tag{6}$$

by ignoring the cylinder's end effects in the limit of $R_0 \ll L_0$. For a balloon having a fixed internal volume $V = \pi R^2 L$, the equilibrium shape is determined by the condition that F is minimized with respect to the λ factors. To write down F as a function of V, a thermodynamic variable conjugate to pressure, we need to invoke the constraint that $\lambda_R^2 \lambda_L$ is constant, equal to $v = V/V_0$, where $V_0 = \pi R_0^2 L_0$ is the initial volume of the balloon. The stretching parameter then takes the form

$$J_1 = \left(1 + \frac{1}{v^2}\right)\lambda_R^2 + \frac{v^2}{\lambda_R^4} - 3 \tag{7}$$

where λ_R is the single variation parameter.

The equilibrium condition $\partial F/\partial \lambda_R = 0$ yields

$$\lambda_R = \left(\frac{2v^4}{1+v^2}\right)^{1/6} \tag{8}$$

which in turn gives

$$\lambda_L = \left(\frac{1+v^2}{2v}\right)^{1/3} \tag{9}$$

$$\lambda_H = \left[\frac{2}{v^2(1+v^2)}\right]^{1/6} \tag{10}$$

Inserting this stationary solution back to Eqs. 3–6, we obtain an explicit expression for F as a function of v

$$F = E_0 f(v) \tag{11}$$

where

$$E_0 = \pi R_0 H_0 L_0 \mu \tag{12}$$

is a system-dependent energy scale. The pressure ΔP needed to inflate the balloon to a size that has volume V is determined by

$$\Delta P = \frac{\partial F}{\partial V} \tag{13}$$

Note that ΔP denotes the difference between pressures inside and outside the balloon.

Equation 13 can be written in a reduced, dimensionless form $\Delta p = \Delta P V_0/E_0 = \Delta P R_0/\mu L_0$, which results in

$$\Delta p = \frac{\partial f(v)}{\partial v} \tag{14}$$

The pressure obtained by this way is illustrated in Figure 2a for a few typical values of J_m. For a system that has a relatively small J_m, Δp rises monotonically, as shown by the curve labeled $J_m = 10$. For a system that has a large J_m, greater than the critical value J_m^*, Δp first increases, reaching a maximum Δp_{S1}; it then decreases reaching a minimum Δp_{S2}, after that, Δp monotonically rises as v increases.

This behavior can be compared with a typical van der Waals gas, where J_m plays the role of the temperature T in a fluid. Figure 2(b) shows a schematic shape of the $\Delta p - v$ curve for a large J_m. A typical $\Delta p - v$ curve contains two spinodal points, labeled as S1 and S2, corresponding to the weakly inflated and inflated branches correspondingly. Their locations are determined by solving

$$\frac{\partial \Delta p}{\partial v} = 0 \tag{15}$$

which produces the two roots, v_{S1} and v_{S2}.

Thermodynamically, when the pressure increases from the weakly inflated region (following the arrow A-B1 in Figure 2b), a first-order phase transition takes place between the two stable states, one weakly inflated (small $v = v_{B1}$) and one inflated (large $v = v_{B2}$). Across the transition, the pressure must be continuous

$$\Delta p(v_{B1}) = \Delta p(v_{B2}) = \Delta p_{co} \tag{16}$$

The work done by inflating the balloon is $(v_{B2} - v_{B1})\Delta p_{cp}$, which must be matched by the change in the Helmholtz energy $f(v_{B1}) - f(v_{B2})$. In other words, the Gibbs free energy must be equal at these points

$$f(v_{B1}) - v_{B1}\Delta p(v_{B1}) = f(v_{B2}) - v_{B2}\Delta p(v_{B2}) \tag{17}$$

Hence, we see that in the current problem, the determination of the phase transition points, v_{B1} and v_{B2}, is fully consistent with the phase transition theory that determines the binodal points of a first-order phase transition.

Within this understanding, this model produces a uniform balloon shape (i.e., R has the same value along the axis) when $v < v_{B1}$ and $v > v_{B2}$. A balloon shape that has a volume v between v_{B1} and v_{S1} can have a uniform R as well; from thermodynamic viewpoint, this shape is only metastable; the metastable state, however, can become quite stable in the current problem, different from the fluid counterpart, which will be addressed in the next subsection.

Here we illustrate the physics of a system with $v_{B1} < v < v_{B2}$. While the thermodynamically stable states can only have v_{B1} or v_{B2}, this means that our system must phase-separate at least into two regions, each has v_{B1} or v_{B2}, so that the overall v is between these two numbers. This situation is similar to the gas–liquid coexistence; below the critical temperature T^*, a fluid system with an overall density between the gas and liquid densities can exist, however, must be accompanied by a gas–liquid interface. We call such a state the biphasic state.

The total free energy of the system for the biphasic state is given by

$$f(v_{B1}, v_{B2}; x) = [xf(v_{B1}) + (1-x)f(v_{B2})] \tag{18}$$

where x $(0 \le x \le 1)$ is the fraction of the weakly inflated region. The constraint $xv_{B1} + (1-x)v_{B2} = v$ relates the three

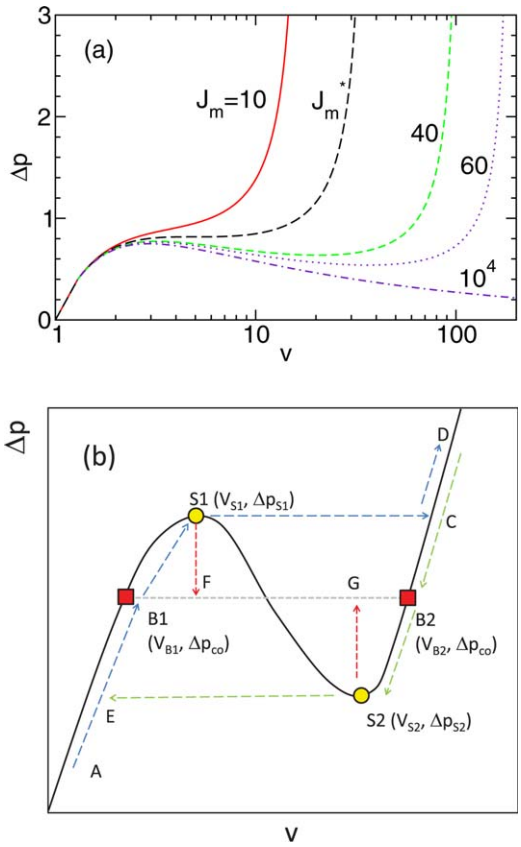

Figure 2. (a) Pressure–volume relation for a few examples of J_m according to the Gent model and (b) the binodal points (squares) and spinodal points (circles) in a typical pressure–volume curve.

The curve labeled J_m^* (=18.231...) in (a) is a critical case, beyond which a maximum Δp_{S1} and a maximum Δp_{S2} in the pressure curve exist. The bionodal points are determined by Eqs. 16 and 17 discussed in the text, with a balance of the pressure (shown by the gray line connecting the two points) and Gibbs free energy. The arrows associated with the dashed lines indicate the hysteresis effects during the inflation-deflation process. In a constant-pressure experiment, the hysteresis loop A-B1-S1-C-D-B2-S2-E is followed; in a constant v experiment, the hysteresis loop A-B1-S1-F-B2-D-B2-S2-G-B1-A is followed. The system is unstable between the two spinodal points labeled S1 and S2. [Color figure can be viewed in the online issue, which is available at wileyonlinelibrary.com.]

parameters $(v_{B1}, v_{B2}; x)$ for a fixed v. In a thermodynamically stable state, we minimize f with respect to v_{B1}, v_{B2}, and x, which gives

$$f'(v_{B1}) = f'(v_{B2}) \tag{19}$$

and

$$f'(v_{B1}) = [f(v_{B1}) - f(v_{B2})]/(v_{B1} - v_{B2}) \tag{20}$$

These conditions are commonly known as the Maxwell condition, or the double-tangent construction condition on the Helmholtz free energy curve. They are fully consistent with Eqs. 16 and 17. The binodal curve determined this way is displayed by the solid curve in Figure 3a; its corresponding pressure, Δp_{co}, is plotted as the solid curve in Figure 3b. The binodal curves v_{B1} and v_{B2} terminates at a critical point v^*. Usually, we determine the critical point by requiring

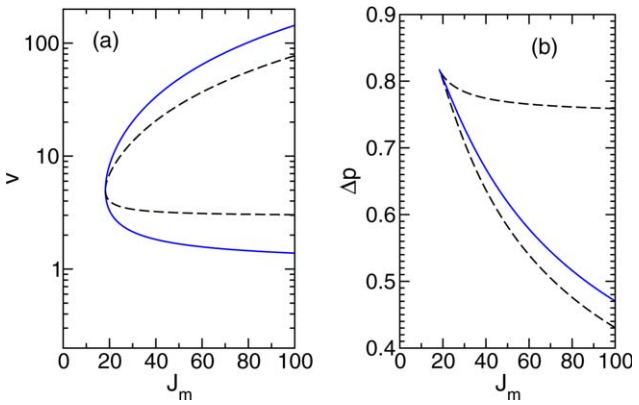

Figure 3. (a) Binodal curves, v_{B1} and v_{B2} (solid curves) and spinodal curves, v_{S1} and v_{S2} (dashed curves), and (b) binodal pressure Δp_{co} (solid curve) and the spinodal pressure Δp_{S1} and Δp_{S2} (dashed curves), determined from the Gent model.

The critical point can be characterized by J_m^*, Δp^*, and v^* given in Eqs. 21 and 22. [Color figure can be viewed in the online issue, which is available at wileyonlinelibrary.com.]

conditions $\partial\Delta p/\partial v=0$ and $\partial^2\Delta p/\partial v^2=0$. The numerical solution to these two equations yields

$$J_m^*=18.231\pm0.001 \quad \text{and} \quad v^*=4.99\pm0.02 \tag{21}$$

which gives

$$\Delta p^*=0.8180\pm0.0001 \tag{22}$$

Hence in this section, we have demonstrated that the structural transition in inflating a balloon is analogous to the gas–liquid transition in fluids. There is one-to-one correspondence of variables in the two systems, with the understanding that J_m plays the same role as the temperature in a gas–liquid transition.

Hysteresis effects in a inflating–deflating process

In this section, we discuss the hysteresis effects and the existence of metastable states in light of the spinodal concept. For a given J_m, in the previous section we already defined the spinodal points, v_{S1} and v_{S2}, at which the pressure reaches maximum and minimum. According to the condition in Eq. 15, we have numerically found the two roots, which are plotted as dashed curves in Figure 3a. The corresponding spinodal pressures, that is, the maximum and minimum in the pressure curve in Figure 2b, are plotted as the dashed curves in Figure 3b.

In fluids, the pressure essentially follows the $P-V$ curve given by the Maxwell construction. Suppose that the volume of a liquid is increased under a constant temperature, the pressure follows the equilibrium $P-V$ curve until it hits the coexistence pressure P_{co}, where the gas phase starts to appear. With further increase of the volume, the pressure remains constant at P_{co} until the whole liquid becomes a gas. After this point, the pressure follows the $P-V$ curve of the gas phase. This is the scenario where we assume that the system can always reach a thermodynamic equilibrium.

In practice, the gas phase may not immediately appear at the pressure P_{co} because an extra work is needed to nucleate a gas volume in a bulk liquid phase. This work, called the nucleation energy, is on the order of the interfacial energy between the gas and liquid phases and is negligibly small compared with the macroscopic energy. Therefore, beyond the binodal point, the system normally makes a phase transition to the other phase, immediately.

Going back to our description of balloon inflation by increasing pressure from a low value, we have already discussed that from point A to point B1 in Figure 2b, the system is thermodynamically stable, where the balloon is weakly inflated along the entire length. As the pressure further increases beyond ΔP_{co}, the system run into a metastable region, from point B1 to S1 in Figure 2b. This is a region where the considered balloon would make a phase separation to at least two regions, corresponding to the weakly inflated and inflated segments. The energy barrier that the system must overcome is again the nucleation energy. At this pressure, the free energy of the coexistent states becomes comparable to that of the uniform state, but a macroscopic work is needed to create the inflated region. Unlike the gas–liquid transition, the nucleation energy in balloons is on the order of a macroscopic energy and is much larger than k_BT. Therefore, a spontaneous transition from the uniform state to biphasic state does not take place at and beyond the pressure ΔP_{co} in normal experimental conditions. We expect that the system follows the $\Delta P-V$ curve all the way to S1.

If we increase the pressure beyond the spinodal point, Δp_{S1}, theoretically $\partial\Delta P/\partial V$ becomes negative and any volume expansion is accompanied by decrease in pressure. Hence, the system becomes unstable and phase transition takes place immediately. With the assumption that the system pressure can be maintained at a constant, Δp_{S1}, by supplying instantaneous inflow of an inflating fluid into the balloon, the entire balloon is inflated, reaching the state labeled C in Figure 2b. After C, the entire balloon becomes inflated uniformly and the pressure increases along the line from C to D.

By repeating the same argument, we can show that when the pressure of the balloon is decreased, the system follows the trajectory labeled by points D, C, B2, S2, E, and A in Figure 2b. Hence, the inflation–deflation processes do not follow the same trajectories and form a hysteresis loop.

Finally, we remark that in the above, we have taken the viewpoint of maintaining a constant external pressure Δp in describing the hysteresis effects. We can also describe a process where the volume inside the balloon is tightly controlled in an experiment. This can be realized by inflating the balloon with an incompressible liquid rather than a compressible gas. The relevant variable is now v and Δp is a derived quantity. As v rises in region $[1, v_{S1}]$ before hitting the spinodal point, the balloon is uniformly inflated, either in the stable or metastable regions. At point S1, if the volume is changed very slowly, the balloon becomes unstable and a inflated segment starts to appear. The pressure decreases along the line S1 to F, now sitting exactly at the coexistence pressure Δp_{co}. This forced phase-separation process creates an interface between the two states. The inflated portion expands as we continuously increase v. Eventually, the system reaches point B2 where the inflated segment dominate the entire balloon. Further increase of v brings us to the uniformly inflated region B2 to D. A reversed process now follows points B, C, B2, S2, G, B1, E, and A in the same plot. The reverse process forms a different hysteresis path from the one described above. This experiment enforces the system to display the biphasic phase when v is in the region between the two spinodal points.

Interfacial Free Energy and Interfacial Width

In the last section, we have described the balloon inflation problem by a free energy model that entails the coexistence of two segments within the same balloon at Δp_{co}: one having weakly inflated diameter and the other having strongly inflated diameter. The region between the two segments forms an interface between these two thermodynamically stable "bulk" phases. In this section, we determine the interfacial shape and the interfacial tension for this system. A few example profiles are shown in Figure 4 where the scaled shape depends on one system-parameter only, J_m.

It is convenient to use a cylindrical coordinate system to attack this problem, where the balloon is assumed to have a central axis coinciding with the Z axis. The inflated balloon shape is described in a parametric form, $Z(s)$ and $R(s)$, where S is a parameter that gives rise to the variation of $Z(S)$ covering the entire region of interest. The initial balloon shape is assumed to have the profile $Z_0(S)$ and $R_0(S)$.

On the basis of analyzing the stretching of a volume element, we can then show that the λ factors take the form

$$\lambda_R(S)=\frac{R(S)}{R_0(S)} \tag{23}$$

and

$$\lambda_L(S)=\left[\frac{\dot{R}^2(S)+\dot{Z}^2(S)}{\dot{R}_0^2(S)+\dot{Z}_0^2(S)}\right]^{1/2} \tag{24}$$

Here, we have followed the convention that a doted function represents the first derivative. In addition, we assume that the constraint in Eq. 1 is always satisfied, now locally

$$\lambda_L(S)\lambda_R(S)\lambda_H(S)=1 \tag{25}$$

which is directly incoorporated in our model by writing λ_H as a function of the other two factors. Hence, the inflation parameter J_1 in Eq. 3 is a function of S.

The Helmholtz free energy functional can then be written as

$$F[\lambda_R(S),\lambda_L(S)]=\pi\mu\int_{-b/2}^{+b/2}\mathrm{d}S R(S)H(S)[\dot{R}^2(S)+\dot{Z}^2(S)]^{1/2}f(\lambda_R,\lambda_L) \tag{26}$$

where f is the Gent model specified in Eq. 5. The parameter b is used here to represent the range of s considered; as described below, the results do not depend on the choice of b, as long as it is asymptotically large. Using the constraint in Eq. 25, the definition of E_0 in Eq. 12, we arrive at

$$F=\frac{E_0}{L_0}\int_{-b/2}^{+b/2}\mathrm{d}S[\dot{R}_0{}^2(S)+\dot{Z}_0{}^2(S)]^{1/2}f(\lambda_R,\lambda_L) \tag{27}$$

The interior balloon volume in a biphasic state can also be written

$$V=\pi R_0^2\int_{-b/2}^{+b/2}\mathrm{d}S\lambda_R^2(S)\dot{Z}(S) \tag{28}$$

For later convenience, we define the Gibbs energy of the system

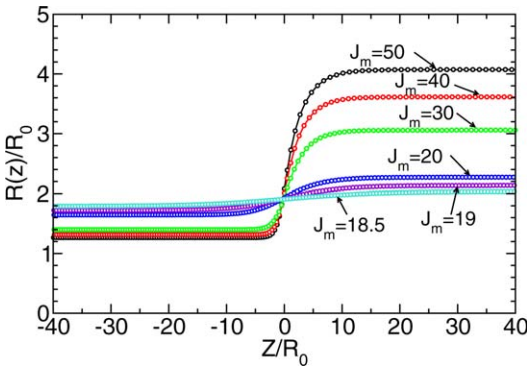

Figure 4. Shape function of the interfacial region between the weakly inflated (left) and strongly inflated (right) regions.

These profiles were produced from a generalized Gent model, which depends on one single system parameter J_m. For comparison, the numerical solutions are overlapped at a point at which the shape curves are steepest. Lines are drawn to connect the actual nodes used in computation, represented by the symbols. [Color figure can be viewed in the online issue, which is available at wileyonlinelibrary.com.]

$$G=F-V\Delta P_{co} \tag{29}$$

which is a functional of the shape function with a given ΔP_{co}. At this stage, the setup of the problem is general, valid for any axisymmetric system of balloon inflation.

We shall consider the biphasic cylindrical balloon problem where a number of simplifications can be made to the formalism. We assume that the original, uninflated balloon can be described by

$$R_0(S)=R_0, \quad \text{and} \quad Z_0(S)=S \tag{30}$$

for $S=[-L_0/2, +L_0/2]$. Combining Eqs. 27–29 we arrive at

$$G=\frac{E_0}{L_0}\int_{-L_0/2}^{+L_0/2}dS[f(\lambda_R,\lambda_L)-\lambda_R^2(S)\dot{Z}(S)\Delta p_{co}] \tag{31}$$

which has a rather simple form. For now, we consider the uniform inflation case to examine consistency; in this special case, both $\lambda_R(S)=\lambda_R$ and $\dot{Z}(S)\equiv\lambda_L$ are constants independent of S. Hence, $G=E_0[f(\lambda_R,\lambda_L)-\lambda_R^2\lambda_L\Delta p_{co}]$. One can show that the minimization of the Gibbs function with respect to λ_L and λ_R reproduces the phase equilibrium conditions in Eqs. 16 and 17. On the basis of solving these equations, we define

$$G_\infty=E_0 g_\infty \tag{32}$$

where $g_\infty=f(v_{B1})-v_{B1}\Delta p_{co}$ is the reduced Gibbs energy, which can be calculated from either coexisting states.

Going back to the calculation for the biphasic case, for convenience, we scale all length parameters by R_0

$$r(s)=R(S)/R_0, \quad z(s)=Z(S)/R_0 \tag{33}$$

where

$$s=S/R_0 \tag{34}$$

We can then show

$$G=\pi R_0^2 H_0 \mu \int_{-\frac{L_0}{2R_0}}^{+\frac{L_0}{2R_0}} ds[f(\lambda_R,\lambda_L)-\lambda_R^2(s)\dot{z}(s)\Delta p_{\rm co}] \qquad (35)$$

Note that at this stage, G is directly proportional to the original length of the cylindrical balloon, L_0, through the limits of the integral over s.

The interfacial tension is defined as the difference between the Gibbs free energy of the biphasic state and the Gibbs free energy of a reference bulk state. Hence, we have

$$\Sigma \equiv G-G_\infty=\pi R_0^2 H_0 \mu \int_{-L_0/2R_0}^{+L_0/2R_0} ds[f(\lambda_R,\lambda_L)-\lambda_R^2(s)\dot{z}(s)\Delta p_{\rm co}-g_\infty] \qquad (36)$$

On the basis of this expression, we are ready to define a reduced surface tension and push L_0/R_0 to infinity

$$\sigma \equiv \Sigma/(\pi R_0^2 H_0 \mu)=\int_{-\infty}^{+\infty} ds[f(\lambda_R,\lambda_L)-\lambda_R^2(s)\dot{z}(s)\Delta p_{\rm co}-g_\infty] \qquad (37)$$

As expected, the surface tension is a property of the interface, hence does not depend on the original balloon length L_0. At this stage, in the reduced version, this functional depends on two undetermined shape functions $\lambda_R(s)$ and $z(s)$. Note that $\lambda_L(s)$ can now be written as $\lambda_L(s)=\{[\dot{\lambda}_R(s)]^2+[\dot{z}(s)]^2\}^{1/2}$.

To minimize the functional σ with respect to these functions, one can follow the standard procedure of writing down the Lagrange–Euler equations for function $\lambda_R(s)$ and $z(s)$, and proceed in solving these differential equations. Note that the integrant does not depend on $z(s)$ directly; therefore, a first-integral can already be found. Here, we take a simple approach. In our numerical solution to the problem, we cut the s space by N equally spaced slabs and represent each of these two functions by N unknown variables, $\lambda_{R1}, \lambda_{R2}, \ldots \lambda_{RN}$ and $z_1, z_2, \ldots, z_N$. The original functional in Eq. 37 is expressed as a function of these $2N$ variables. The final expression for σ is then fed into a computer code that solves the multivariable minimization problem. The procedure is efficient if one provides a good initial guess of the profile. In our case, a smooth function that connects the left side of the cylindrical balloon to the right side was used. All results presented in this article were based on $N = 256$.

One can verify that the only physical parameter in this interfacial problem is $J_{\rm m}$, after we write all quantities in reduced units. Figure 4 shows the phase profile of the interface obtained this way, where the left hand side corresponds to the B1 phase and the right hand side B2. As $J_{\rm m}$ increases, the difference between the inflated and weakly inflated regions becomes more profound, and the interfacial width decreases. This tendency is similar to what we see in the gas–liquid interface. As we approach the critical point (represented by T^* for fluids and $J_{\rm m}^*$ for balloons), the volume difference between the coexistent states becomes less and the interfacial thickness increases. Note that in the current problem, the interfacial profile is not symmetric with respect to a central point; we use the point where the interface curve shows the largest slope as $Z = 0$ in these plots; the left and right wings of the profiles change asymmetrically about this point.

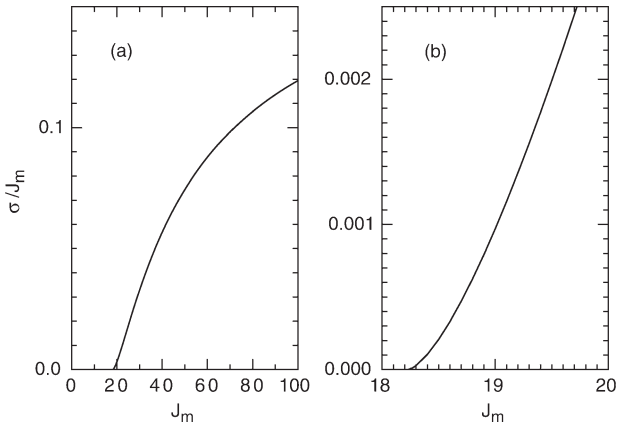

Figure 5. Reduced interfacial free energy σ as a function of the system parameter $J_{\rm m}$ in the (a) full and (b) near-critical regions.

The reduced interfacial tension σ is displayed in Figure 5 as a function of the system dependent parameter $J_{\rm m}$. As can be seen from plot (b), near the critical point, as $J_{\rm m}$ approaches from the high side to the critical point $J_{\rm m}^*$, σ approaches zero linearly. This is consistent with the power law

$$\sigma \propto (J_{\rm m}-J_{\rm m}^*)^{2\nu} \qquad (38)$$

where the critical exponent $\nu=1/2$ in a mean-field theory; this power law can be compared with the current understanding of the interfacial tension near the critical point T^* in a fluid system.

There are various theoretical definitions of the interface width W. Here, we adopt the definition

$$R_0/W=\mathrm{Max}\left[\frac{d}{dz}\left(\frac{r(z)}{(r_{\rm B2}-r_{\rm B1})}\right)\right] \qquad (39)$$

which can be easily accessed in the numerical solution. The function Max takes the maximum value of its argument. The inverse of the interfacial width R_0/W is shown in Figure 6. As the critical point $J_{\rm m}^*$ is approached, this quantity approaches zero following the behavior

$$R_0/W \propto (J_{\rm m}-J_{\rm m}^*)^{\nu} \qquad (40)$$

The critical exponent $\nu=1/2$ is typical in the mean-field theory treatment of the critical phenomenon in fluids.

Discussion and Conclusions

In this article, we studied the inflation problem of a cylindrical balloon, on the basis of the Gent model, which is suitable for describing the deformation of rubber material. We showed that the system displays a behavior similar to the gas–liquid transition of a simple fluid. A phase diagram was constructed in the parameter space of pressure vs. volume, where the spinodal curve, binodal curve, and critical point can all be identified, similar to those predicted from the van der Waals theory.

As the balloon is inflated going through a biphasic state, the interface between the inflated and weakly inflated regions was also discussed. We showed that the interface displays the same tendency as in a gas–liquid coexistence system; as the critical point is approached, the interfacial thickness

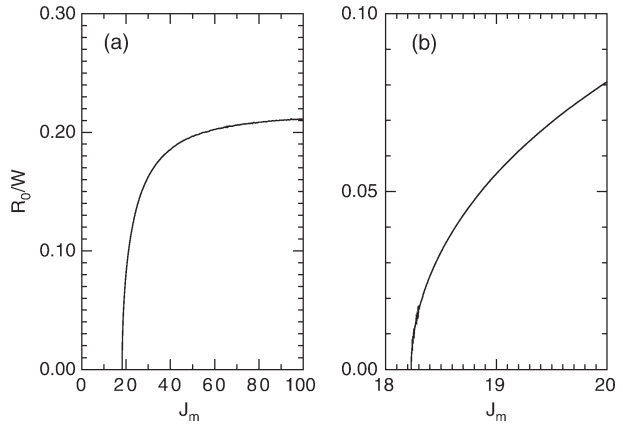

Figure 6. Reduced inverse interfacial width R_0/W as a function of J_m in the (a) full and (b) near-critical regions.

increases and the interfacial energy decreases. A complete numerical solution to the problem was presented.

Conversely, it must be noted that there are differences between the properties of balloon inflation and gas–liquid transition. One notable point is that in the current system, the thermal energy plays no role, and there are strong hysteresis effects which are discussed in the hysteresis section. This is caused by the nucleation energy barrier that is no longer small in our system. The existence of a macroscopic interface in the current system provides us a unique opportunity to access the interfacial properties such as the shape function. It would be rewarding to directly probe the interfacial properties in the current system experimentally.

There is other important difference which has not been addressed in this article. Balloon is an elastic material, and its free energy depends on the shape of the balloon in the force free state. The present discussion holds for a long cylindrical balloon, and would not necessarily hold for balloons having other shapes. Taking the case of a spherical balloon for instance, we can develop the same story for the $\Delta P-V$ curve, similar to the discussion presented in previous section, where we can determine the binodal and spinodal curves. However, the spherical shape remains locally stable in the region between the spinodal points. Therefore, the pressure in spherical balloons follows the $\Delta P-V$ calculated for a uniform, spherical state: a biphasic state does not exist.

In this article, we have used the Gent model to study the current system. There are two basic criteria in the model. (a) In a weakly deformed state, the model recovers the Neo-Hookian model and (b) in the strongly deformed state, the model yields an upper limit which forbids the system to further stretch. We have attempted other simple function forms of the stretching energy that meet these two criteria. They all show a qualitatively similar phase behavior to that of the Gent model discussed in this article. Therefore, our observed phase behavior is intrinsic to rubber material, independent of the actual theoretical model of the stretching energy, as long as the model satisfies these criteria.

Acknowledgments

This work was supported by NSFC under grant numbers 31128004, 91027045, 10834014, and 11175250. FLM thanks the financial support from the National Basic Research Program of China (973 program, No. 2013CB932800). JZYC thanks the financial support from the National Science and Engineering Research Council of Canada.

Literature Cited

1. Mallock A. Note on the instability of India-rubber tubes and balloons when distended by fluid pressure. *Proc R Soc Lond.* 1890;49: 458–463.
2. Kyriakides S, Chang Y. The initaiation and propagation of a localized instability in an inflated elastic tube. *Int J Solids Struct.* 1990; 26(9–10):975–991.
3. Hill JM, Milan AM. Finite elastic non-symmetrical inflation and eversion of circular cylindrical rubber tubes. *Proc R Soc Lond A.* 1999;455(1983):1067–1082.
4. Gonçalves PB, Pamplona D, Lopes SRX. Finite deformations of an initially stressed cylindrical shell under internal pressure. *Int J Mech Sci.* 2008;50(1):92–103.
5. Müller I, Strehlow P. *Rubber and Rubber Balloons, Paradigms of Thermodynamics*. Lecture Notes in Physics, Vol. 637. Berlin: Springer-Verlag, 2004.
6. Gent AN. Elastic instabilities in rubber. *Int J Nonlinear Mech.* 2005; 40(2–3):165–175.
7. Treloar LRG. *The Physics of Rubber Elasticity*, 3rd ed. Oxford University Press: Oxford, 2005.
8. Gent AN. A new constitutive relation for rubber. *Rubber Chem Technol.* 1996;69(1):59–61.

Manuscript received Sept. 30, 2013, and revision received Dec. 17, 2013.